



Heriot-Watt University
Research Gateway

White powder identification using broadband coherent light in the molecular fingerprint region

Citation for published version:

Maidment, L, Schunemann, PG & Reid, DT 2018, 'White powder identification using broadband coherent light in the molecular fingerprint region', *Optics Express*, vol. 26, no. 19, pp. 25364-25369.
<https://doi.org/10.1364/OE.26.025364>

Digital Object Identifier (DOI):

[10.1364/OE.26.025364](https://doi.org/10.1364/OE.26.025364)

Link:

[Link to publication record in Heriot-Watt Research Portal](#)

Document Version:

Publisher's PDF, also known as Version of record

Published In:

Optics Express

Publisher Rights Statement:

Published by The Optical Society under the terms of the Creative Commons Attribution 4.0 License. Further distribution of this work must maintain attribution to the author(s) and the published article's title, journal citation, and DOI.

General rights

Copyright for the publications made accessible via Heriot-Watt Research Portal is retained by the author(s) and / or other copyright owners and it is a condition of accessing these publications that users recognise and abide by the legal requirements associated with these rights.

Take down policy

Heriot-Watt University has made every reasonable effort to ensure that the content in Heriot-Watt Research Portal complies with UK legislation. If you believe that the public display of this file breaches copyright please contact open.access@hw.ac.uk providing details, and we will remove access to the work immediately and investigate your claim.



White powder identification using broadband coherent light in the molecular fingerprint region

LUKE MAIDMENT,^{1,2} PETER G. SCHUNEMANN,³ AND DERRYCK T. REID^{1,*}

¹ *Scottish Universities Physics Alliance (SUPA), Institute of Photonics and Quantum Sciences, School of Engineering and Physical Sciences, Heriot-Watt University, Edinburgh EH144AS, UK*

² *Chromacity Ltd., 43 Discovery Terrace, Research Avenue North, Riccarton, Edinburgh EH144AP, UK*

³ *BAE Systems, Inc., MER15-1813, P.O. Box 868, Nashua, NH, USA 03061-0868*

**D.T.Reid@hw.ac.uk*

Abstract: We show that a variety of white powder samples, including painkillers, amino acids, stimulants and sugars are readily discriminated by diffuse reflectance infrared spectroscopy involving no preparation of the sample and no physical contact with it. Eleven powders were investigated by illuminating each sample with broadband coherent light in the 8–9- μm band from an OPGaP femtosecond optical parametric oscillator. The spectra of the scattered light were obtained using Fourier-transform spectroscopy. Similarities between different spectra were quantified using Pearson's correlation coefficient, confirming that spectral features in the 8–9- μm wavelength region were sufficient to discriminate between all eleven powders evaluated in the study, offering a route to simple and automated non-contact chemical detection.

Published by The Optical Society under the terms of the [Creative Commons Attribution 4.0 License](#). Further distribution of this work must maintain attribution to the author(s) and the published article's title, journal citation, and DOI.

1. Introduction

Various agendas motivate the identification of white powders, such as detecting counterfeit pharmaceuticals [1,2] and foodstuff analysis [3]. Raman and Fourier-transform spectroscopy (FTS) can discriminate between materials according to their chemistry and crystallography, expressed by characteristic absorption signatures in the 6–12 μm region (833–1667 cm^{-1}). Typically, FTS of powders proceeds via the attenuated total internal reflection (ATR) method [4], in which intimate contact between a solid sample and the ATR cell is ensured by applying high pressure. ATR is an established field technique [5] but encounters certain limitations [6], and crucially requires contact between the sample and the ATR interface, risking sample contamination or exposing a user to hazardous materials. By contrast, diffuse reflectance FTS needs no sample preparation and is a non-contact method, but is difficult to implement with the spatially incoherent thermal sources utilized in ATR embodiments. Raman spectroscopies face other constraints due to the weak cross-sections of spontaneous Raman scattering, or the complexity of more sensitive methods like coherent anti-Stokes Raman spectroscopy [7].

Spatially coherent broadband mid-infrared (mid-IR) sources have seen significant recent development, particularly in the molecular fingerprint region. The narrow spectra from external cavity quantum cascade lasers (EC-QCLs) can be rapidly and widely tuned (e.g. 7.7–10.1 μm in [8]), and QCL arrays can cover from 6.5 to 11 μm in a small package for standoff detection [9]. An EC-QCL system has been used to identify bulk powders like paracetamol by collecting diffuse reflectance spectra at a range of 1 m, and identifying trace amounts of powdered explosive residue [10]. New nonlinear materials like orientation-patterned gallium phosphide [11] (OPGaP) avoid the multi-phonon IR absorptions associated with oxide materials such as LiNbO_3 , allowing the generation of wavelengths $\gg 5 \mu\text{m}$. Notably, the femtosecond OPGaP optical parametric oscillator (OPO) we reported previously [12]

produces spectra with bandwidths of 200–1000 nm, tunable from 5 to 13.5 μm [13], enabling novel spectroscopies in the molecular fingerprint band including dual-comb spectroscopy [14,15] and standoff aerosol spectroscopy [16,17]. The spatially coherent nature of the OPGaP OPO, together with its high average power (up to 100 mW from 5 to 9 μm) enables identification of solids and liquids in a FTS modality that works by scattering the beam from the sample surface, avoiding the physical contact present in ATR cells. Diagnostically useful information does not demand high resolution—liquids and solids exhibit wide absorption features, so cm^{-1} -level resolution is sufficient—but unique identification makes it important to capture information over several hundred cm^{-1} , making femtosecond sources well suited due to their broad spectra. Here, we present an application of such OPOs in the identification of white powders, benefiting from their spatial coherence and high average power.

2. Active illumination Fourier-transform spectrometer

The spectroscopic approach we employed is illustrated in Fig. 1 and is similar to that described in greater detail in [16,18,19]. The mid-IR beam (diameter 5 mm) from an OPGaP femtosecond OPO [12] was directed through a scanning Michelson interferometer (acting as a Fourier-transform spectrometer) before being incident on the powder sample. Separate detectors recorded the interferograms of the HeNe calibration laser (Si photodiode) and the IR laser pulses before and after the sample (cryogenically cooled HgCdTe detectors). The spectrum of the 200-fs-duration mid-IR pulses was obtained after calibrating the mid-IR interferogram delay axis using the HeNe interferogram, then performing a Fourier transform.

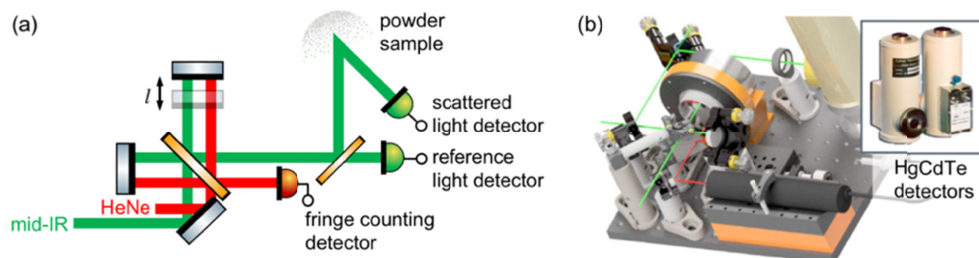


Fig. 1. (a) Scanning Michelson interferometer used to modulate the OPO idler beam (green) and the HeNe displacement-calibration beam (red). (b) Actual layout, with voice-coil actuator.

After the interferometer, around 15 mW of mid-IR light was directed onto a small heaped powder sample with a mass of ~ 10 g; examples are shown in Figs. 2(a) and 2(b). No effort was made to control the shape of the powder, which was presented on top of a piece of thin card. The mid-IR light illuminated the powder sample along a direction normal to the card, with the diffuse light scattered over the full range of solid angles, which we exploited by collecting light scattered at $\sim 90^\circ$ to the incident beam. This light was focused on a HgCdTe detector using a lens system consisting of a 50-mm diameter, 100-mm focal length ZnSe lens to collect the scattered light and a 25-mm Ge lens to focus to the detector element [Fig. 2(c)].

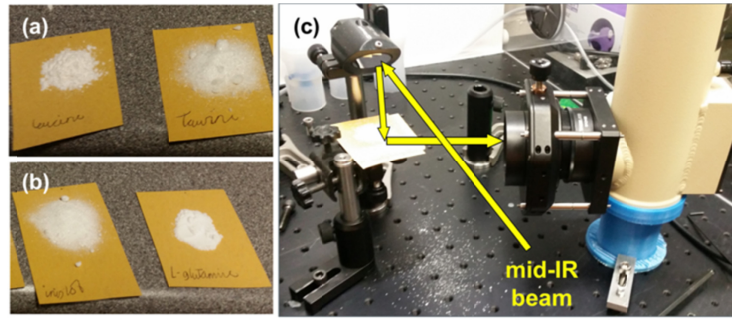


Fig. 2. (a,b) Prepared powder samples, and (c) illumination geometry used in the experiment.

To illustrate the approach for obtaining the spectral response of a powder, we show in Fig. 3. spectra of the light scattered from caffeine powder illuminated by broadband 8–11 μm radiation generated using OPGaP gratings with periods $\Lambda = 29 \mu\text{m}$, $31 \mu\text{m}$ and $32.5 \mu\text{m}$. The spectra of the illumination and scattered light are shown in Fig. 3(a), each one based on an average of seven measurements recorded in 250 ms at 2-cm^{-1} resolution. The scattered spectrum in each case is divided by the illumination spectrum to find the spectral response of the powder, shown in Figs. 3(b)–3(d), revealing clear distinguishing absorption features.

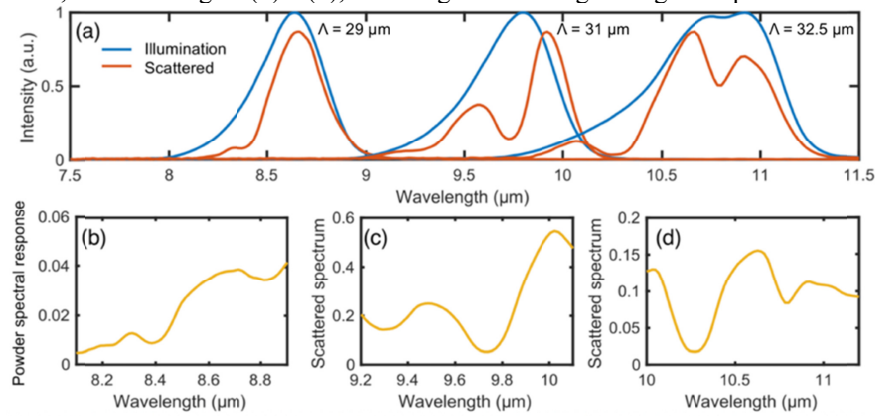


Fig. 3. (a) Illumination spectra from three OPGaP grating periods (blue), and scattered from caffeine powder (red). (b–d) Spectral response (ratio of scattered / illumination spectra).

3. Library data set construction and analysis

A library of powder response spectra was compiled by collecting 14 interferograms of 11 white powder samples using the 29- μm grating. The powders chosen were readily available painkillers, nutritional supplements (amino acids), a stimulant and a simple sugar. Figure 4 presents the complete list. These powders were selected for their potential similarities and because they required no special handling precautions. Examples of the library spectra recorded using the 29- μm grating from 8.2 to 8.9 μm are shown in Columns 1 and 3 of Fig. 4.

Pearson's correlation coefficient [20] reports the similarity between two spectra, X_i and Y_i :

$$r = \frac{\sum_{i=1}^n (X_i - \bar{X})(Y_i - \bar{Y})}{\sqrt{\sum_{i=1}^n (X_i - \bar{X})^2} \sqrt{\sum_{i=1}^n (Y_i - \bar{Y})^2}} \quad (1)$$

This correlation coefficient is particularly suited to our purpose because it is insensitive to differences in the absolute magnitude of the compared spectra, but recognizes the shape and position of features, returning a maximum value of 1 for perfect correlation, and -1 for

perfect anti-correlation. Correlating the library with itself gives a first indication of the potential of this metric to distinguish powders from their spectral responses. In Fig. 5 we show the results of such an operation, with the high contrast between the on-diagonal and off-diagonal components showing that Pearson's correlation coefficient offers a practical means of discrimination.

To test how effectively Pearson's correlation coefficient could be used to identify a powder from an independently measured test spectrum, its correlation coefficient with respect to every library spectrum was found, and the correlation values for each particular chemical averaged, giving a single correlation value between a test spectrum and each powder (Fig. 4, red text). This approach identified the best match to be the chemical with the highest averaged correlation coefficient and worked well to classify any individual spectrum recorded at the same time as the library data was recorded, as illustrated in Columns 2 and 4 of Fig. 4.

The experiment was repeated using test data recorded with fresh samples of the same powders. The signal strengths of these data were $2 \times$ weaker than the library data. Table 1 presents representative results, displaying the mean correlation coefficient of three tests with each library chemical. Taurine and L-glutamine were matched correctly, while creatine was poorly matched, with a correlation coefficient equal to the taurine library data.

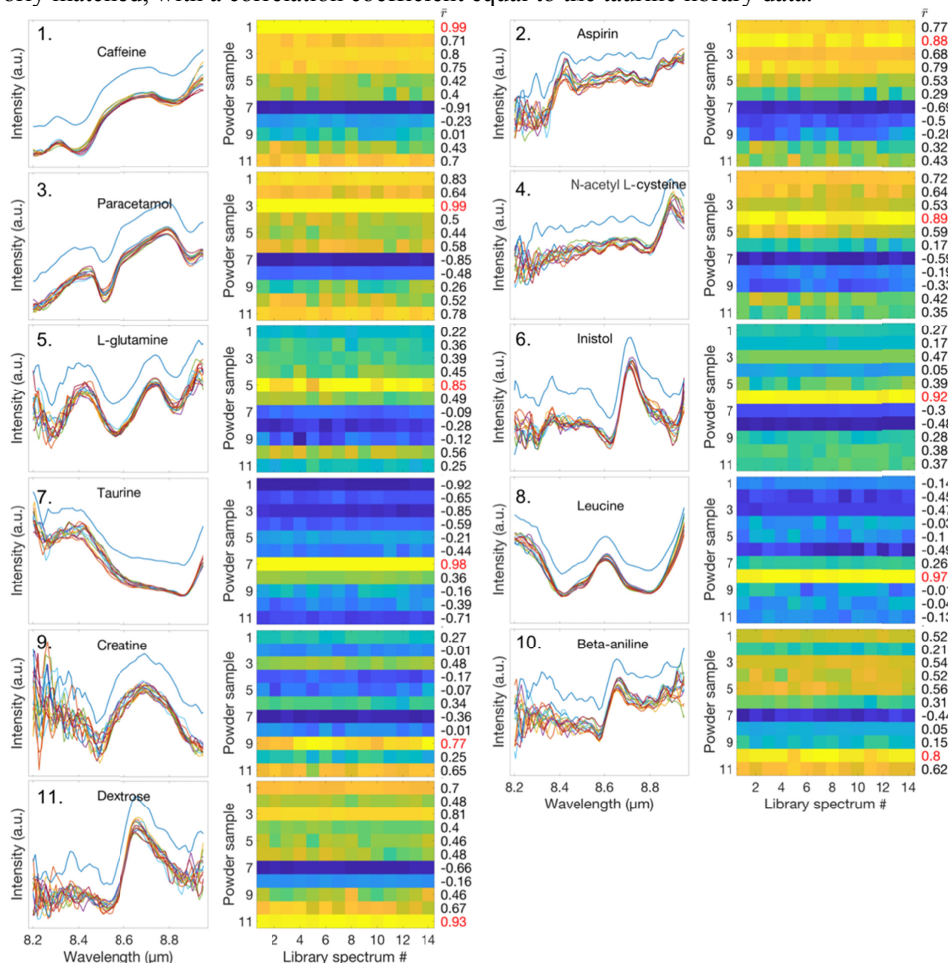


Fig. 4. Columns 1, 3: Library spectra derived from 14 pairs of illumination- and scattered-light spectra and (offset) independently measured test spectrum for each of 11 powders. Columns 2, 4: Pearson's correlation coefficients between each test spectrum and every member of the library data set, showing a consistent maximum average correlation coefficient (red) when the test and library spectra correspond to the same powder.

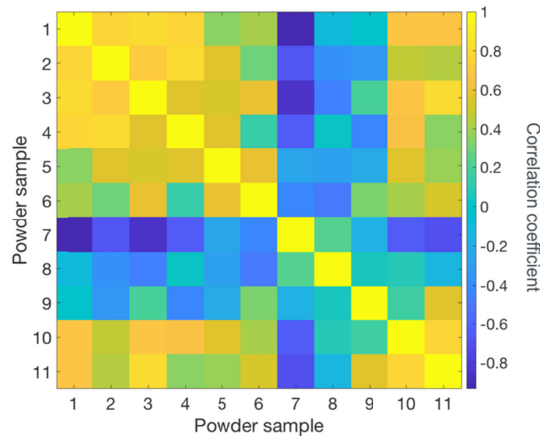


Fig. 5. Correlation coefficients computed between the averaged spectral responses of the library spectra. The values of all the off-diagonal elements are much less than one, indicating the suitability of Pearson's correlation coefficient as a metric to distinguish between spectra.

Table 1. Mean correlation coefficients of taurine, L-glutamine and creatine powders with library powders. Conclusive matching is shown in green, inconclusive in red. Powders with all coefficients < 0.5 are omitted.

Test powders	Taurine	L-glutamine	Creatine
Caffeine	-0.96	0.53	-0.57
Aspirin	-0.70	0.51	0.40
Paracetamol	-0.89	0.52	-0.40
N-acetyl L-cysteine	-0.72	0.69	-0.70
L-glutamine	-0.44	0.89	-0.45
Taurine	0.95	-0.36	0.53
Creatine	-0.06	-0.26	0.53
Beta-aniline	-0.52	0.61	-0.22

The spectrum of light scattered by a powder depends on the complex refractive index of the material, as well as the particle size distribution (due to Mie scattering) [21]. A similar problem is encountered in standoff detection of liquids, where the measured spectrum can be absorption, reflection or substrate dominated [9]. It remains to be tested whether using the same library to analyze chemically identical powder samples with different particle size distributions will work, because particle-size-dependent scattering may alter the scattered spectrum.

4. Summary and conclusions

Here, we have shown how visually indistinguishable powder samples can be identified by means of diffuse reflectance spectroscopy conducted using coherent broadband mid-IR light from an OPGaP OPO. Using illumination from only a single OPGaP grating period and an automated classification approach, we could identify powders from spectra with distinctive features between 8.2 and 8.9 μm , even when measurements were repeated with significantly weaker signals. Diagnostic features were observed in the IR response spectra from all the powders under test by observing diffusely reflected light from the surface of the powder. Using broadband light eliminates laser speckle from the measurements but may expose étalon effects in the system, such as those from thin windows on detectors.

By extending the library across a greater wavelength range, it should be possible to measure scattering over a wavelength range of sufficient extent to enable a variety of materials to be identified, with applications in security screening, forensics and production control. An area for further investigation would be to examine the reliability of the Pearson's correlation technique in the presence of a mixture of two or more powders.

5. Funding

DSTL (DSTLX-1000084801, DSTLX-1000106564); EPSRC (EP/L01596X/1).

References

1. A. K. Deisingh, "Pharmaceutical counterfeiting," *Analyst (Lond.)* **130**(3), 271–279 (2005).
2. S. Neuberger and C. Neusüß, "Determination of counterfeit medicines by Raman spectroscopy: Systematic study based on a large set of model tablets," *J. Pharm. Biomed. Anal.* **112**, 70–78 (2015).
3. W.-H. Su and D.-W. Sun, "Fourier transform infrared and raman and hyperspectral imaging techniques for quality determinations of powdery foods: a review," *Compr. Rev. Food Sci. Food Saf.* **17**(1), 104–122 (2018).
4. S. G. Kazarian and K. L. Chan, "Micro- and macro-attenuated total reflection Fourier transform infrared spectroscopic imaging. Plenary Lecture at the 5th International Conference on Advanced Vibrational Spectroscopy, 2009, Melbourne, Australia," *Appl. Spectrosc.* **64**(5), 135A–152A (2010).
5. Smiths Detection, "HazMatID," <https://www.smithsdetection.com/products/hazmatid-elite/>.
6. J. Grdadolnik, "ATR-FTIR spectroscopy: its advantages and limitations," *Acta Chim. Slov.* **49**, 631–642 (2002).
7. G. Rasskazov, A. Ryabtsev, and M. Dantus, "Eye-safe near-infrared trace explosives detection and imaging," *Opt. Express* **25**(6), 5832–5840 (2017).
8. R. Ostendorf, L. Butschek, S. Hugger, F. Fuchs, Q. Yang, J. Jarvis, C. Schilling, M. Rattunde, A. Merten, J. Grahmann, D. Boskovic, T. Tybussek, K. Rieblinger, and J. Wagner, "Recent advances and applications of external cavity-QCLs towards hyperspectral imaging for standoff detection and real-time spectroscopic sensing of chemicals," *Photonics* **3**(2), 28 (2016).
9. M. F. Witniski, R. Blanchard, C. Pfluegl, L. Diehl, B. Li, K. Krishnamurthy, B. C. Pein, M. Azimi, P. Chen, G. Ulu, G. Vander Rhodes, C. R. Howle, L. Lee, R. J. Clewes, B. Williams, and D. Vakhshoori, "Portable standoff spectrometer for hazard identification using integrated quantum cascade laser arrays from 6.5 to 11 μm ," *Opt. Express* **26**(9), 12159–12168 (2018).
10. L. Butschek, S. Hugger, J. Jarvis, M. Haertelt, A. Merten, M. Schwarzenberg, J. Grahmann, D. Stothard, M. Warden, C. Carson, J. Macarthur, F. Fuchs, R. Ostendorf, and J. Wagner, "Microoptoelectromechanical systems-based external cavity quantum cascade lasers for real-time spectroscopy," *Opt. Eng.* **57**(01), 011010 (2017).
11. L. A. Pomeranz, P. G. Schunemann, D. J. Magarrell, J. C. McCarthy, K. T. Zawilski, and D. E. Zelmon, "1- μm -pumped OPO based on orientation-patterned GaP," *Proc. SPIE* **9347**, 93470 (2015).
12. L. Maidment, P. G. Schunemann, and D. T. Reid, "Molecular fingerprint-region spectroscopy from 5 to 12 μm using an orientation-patterned gallium phosphide optical parametric oscillator," *Opt. Lett.* **41**(18), 4261–4264 (2016).
13. L. Maidment, O. Kara, P. G. Schunemann, J. Piper, K. McEwan, and D. T. Reid, "Long-wave infrared generation from femtosecond and picosecond optical parametric oscillators based on orientation-patterned gallium phosphide," *Appl. Phys. B* **124**(7), 143 (2018).
14. O. Kara, L. Maidment, T. Gardiner, P. G. Schunemann, and D. T. Reid, "Dual-comb spectroscopy in the spectral fingerprint region using OPGaP optical parametric oscillators," *Opt. Express* **25**(26), 32713–32721 (2017).
15. H. Timmers, A. Kowligy, A. Lind, F. C. Cruz, N. Nader, M. Silfies, G. Ycas, T. K. Allison, P. G. Schunemann, S. B. Papp, and S. A. Diddams, "Molecular fingerprinting with bright, broadband infrared frequency combs," *Optica* **5**(6), 727–732 (2018).
16. L. Maidment, Z. Zhang, C. R. Howle, and D. T. Reid, "Stand-off identification of aerosols using mid-infrared backscattering Fourier-transform spectroscopy," *Opt. Lett.* **41**(10), 2266–2269 (2016).
17. L. Maidment, P. G. Schunemann, R. J. Clewes, M. D. Bowditch, C. R. Howle, and D. T. Reid, "Systematic spectral shifts in the mid-infrared spectroscopy of aerosols," *Opt. Express* **26**(15), 18975–18981 (2018).
18. D. T. Reid, O. Kara, M. Rutkauskas, and L. Maidment, "Chemical detection using broadband femtosecond optical parametric oscillators in the 6–12- μm spectral fingerprint region," *Proc. SPIE* **10639**, 106392D (2018).
19. L. Maidment, R. A. McCracken, O. Kara, P. G. Schunemann, and D. T. Reid, "Identification of white powder samples using broadband coherent light in the molecular fingerprint region," in *Conference on Lasers and Electro-Optics, OSA Technical Digest (Optical Society of America, 2018)*, paper ATh4O.6.
20. M. Kumar, M. N. Islam, F. L. Terry, Jr., M. J. Freeman, A. Chan, M. Neelakandan, and T. Manzur, "Stand-off detection of solid targets with diffuse reflection spectroscopy using a high-power mid-infrared supercontinuum source," *Appl. Opt.* **51**(15), 2794–2807 (2012).
21. R. Furstenberg, C. A. Kendziora, M. R. Papantonakis, V. Nguyen, and R. A. McGill, "The challenge of changing signatures in infrared stand-off detection of trace explosives," *Proc. SPIE* **9073**, 90730M (2014).